WARSAW UNIVERSITY OF TECHNOLOGY Index 351733
FACULTY OF CIVIL ENGINEERING
COMMITTEE FOR CIVIL AND WATER ENGINEERING
POLISH ACADEMY OF SCIENCES ISSN 1230-2945

DOI: 10.24425/ace.2021.138072

ARCHIVES OF CIVIL ENGINEERING

Vol. LXVII ISSUE 3 2021

s. 581–597

Research paper

Influence of vertical ground motion on seismic responses of triple friction pendulum interlayer isolation structures

Z. Fang[1], P. Yan[2]

Abstract: In order to investigate the influence of vertical ground motion on seismic responses of story-isolation structures mounted on triple friction pendulum (TFP) bearings, the finite element model of a six-story building with various types of interlayer isolation TFP bearings under far field or near fault ground motions is established and analysed. A discrepancy rate function of peak interlayer shear, acceleration and displacement results is adopted to discuss the influence of the vertical seismic motions on isolation structural responses. Furthermore, the isolation form, the isolation period and the friction coefficient of bearings are changed to study their effect on the vertical seismic component's influence. The results show that the influence of the vertical seismic component is considerable on the isolation layer especially under near-fault ground motions, so it should not be overlooked during the structural design; The change of isolation forms will greatly affect the influence of the vertical seismic component especially in the isolation layer and isolation systems with isolation devices set on higher stories or with less isolation layers will have less vertical seismic effect on story acceleration; The increase of the isolation period will globally result in the decrease of the influence of vertical seismic components, though in some cases it shows some sort of fluctuation before the final decrease; The increase of the friction coefficient will lead to the global decrease in the influence of the vertical seismic component in single-layer isolation structures, while it does not obviously affect those in the multi-layer isolation systems.

Keywords: vertical ground motion; interlayer isolation structures; seismic responses; triple friction pendulum

[1] PhD., Nanjing Institute of Technology, School of Architecture Engineering, Hongjing Avenue 1, 211167 Nanjing, China, e-mail: phoenix.fang@hotmail.com

[2] Master, Jiangsu Provincial Architectural D&R Institute LTD, Chuangyi Road 86, 211167 Nanjing, China, e-mail: pingyan220151110@outlook.com

1. Introduction

Earthquakes with great destructive effect may seriously endanger human life and property. Currently base isolation technology using isolators such as flat sliders and pendulum bearings is an effective way to resist earthquake damage. Among them, the triple friction pendulum (TFP) is the recent advance, which has one slider on four spherical sliding surfaces as shown in Fig.1. Although base isolation is the current main form of seismic isolation, it is usually utilized in new buildings and shows great difficulty in building retrofit engineering cases due to expensiveness and complexity in construction. As a result, the interlayer isolation technology whose isolators are installed on higher floors with advantages of convenient construction and economy shows a promising future. Ryan and Earl [1] imagined the effectiveness of interlayer isolation systems as a function of their location and explored alternative approaches for the selection of their properties; Charmpis et al. [2] optimized the seismic responses of multi-layer buildings with seismic isolation at various height; Fakhri and Amiri [3] conducted the nonlinear time-history analysis of interlayer building isolated with TFP bearings and found that the base and first-story isolation systems were extremely effective in the reduction of maximum drift ratio and story shear force. Reggio and Angelis [4] optimized the interlayer isolation with non-conventional TMD.

It is clear from the above review that though the seismic response of interlayer isolation buildings under horizontal ground motion has been studied a lot, there are few research discussing that under the vertical ground motion. A few detailed discussions on the effect of seismic vertical component on responses of friction pendulum base isolation structures have been made. For example, Rabiei and Khoshnoudian [5], [6] considered the vertical component of earthquakes in the analysis of single concave friction pendulum base-isolated buildings and also the double concave friction pendulum base-isolated structures; Loghman et al. [7] demonstrated that the maximum error in determining the base shear caused by neglecting the vertical component of an earthquake was 29.5% for triple concave friction pendulum base-isolated structures. However, obviously the above research is limited to the discussion of base-isolation structures and the conclusions may not be applicable to interlayer isolation structures. As far as the authors' knowledge, the effect of seismic vertical component on responses of TFP interlayer isolation structures has hardly ever been discussed in literature before. So interlayer isolation structures with TFP bearings under seismic excitation considering the vertical ground motion deserves further study.

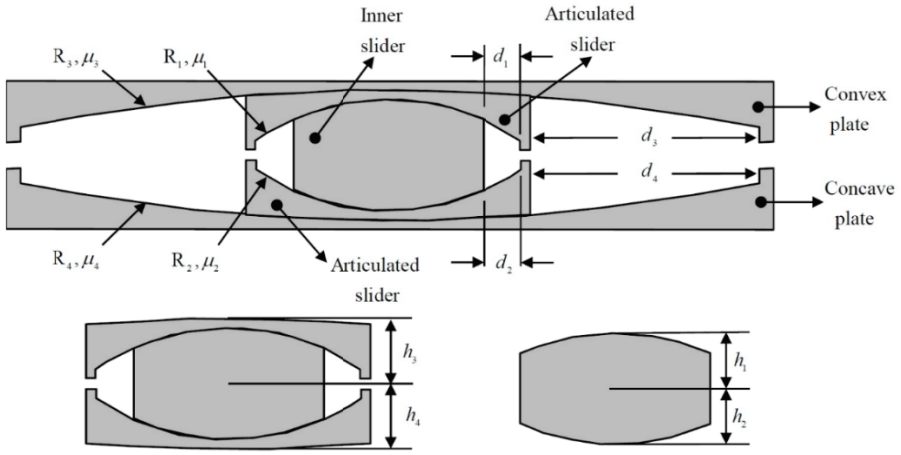

Fig. 1. Cross-section of TFP bearings

In this paper, the effect of vertical ground motions is discussed by taking a six-story building with various forms of interlayer isolation systems by TFP bearings under far field and near fault ground motions as an example, based on the interlayer shear, acceleration and displacement responses. In addition, the influence of various parameters such as isolation forms, isolation periods and friction coefficients on the vertical seismic effect on structural responses is also examined.

2. Simulation and analysis of seismic isolation buildings

The parameters of TFP bearings in this research are summarized in Table 1. The theoretical constitutive behavior of TFP bearings is dependent on the effective radius L_i of each sliding surface i, defined as the difference between the curvature radius of the relevant spherical surface i and the corresponding portion of the height of the slider i, $L_i = R_i - h_i$. The theoretical backbone curve of the designed bearing is shown in Fig. 2a), where a five-stage force-displacement relationship is assumed [8,9]. The numerical model of TFP bearings can be simulated by the assembly of gap elements and single concave FP elements (spring elements and friction elements) [10]. The relationship between these elements are shown in Fig. 2b). Each element group represents the mechanism of a pendulum. The stiffness of the linear spring k_i represents the linear restoring force due to the curvature of the concave plate and the vertical force (k_{ji} means the stiffness of the linear spring at the j-th stage in the i-th element). The friction coefficient of the friction element f_i represents the friction coefficient of the friction surface and the gap distance of the gap element r_{Gi} indicates the limited displacement of the sliding surface. In addition, a normalized force F/W is defined where F is the horizontal force and W is the vertical loading at the sliding surface. The

model developed by Nan Dao [10] is available in the OPENSEES program denoted as "triple friction pendulum" element and it is adopted to simulate the bearings in this research.

Table 1. Parameters of TFP bearings

T_{eff} (s)	ζ_{eff} (%)	$L_1(L_2), L_3(L_4)$ (m)	$d_1(d_2), d_3(d_4)$ (m)	$\mu_1(\mu_2), \mu_3(\mu_4)$
2.5	5.4	0.25,0.85	0.08, 0.48	0.02, 0.08
3.5	11.4	0.384,1.862		
4.5	20.3	0.384,3.709		
5.5	30.7	0.6,7.57		

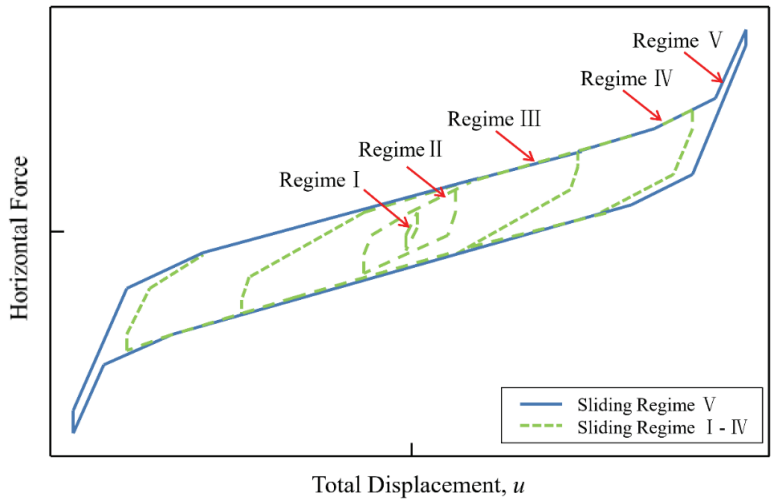

a)

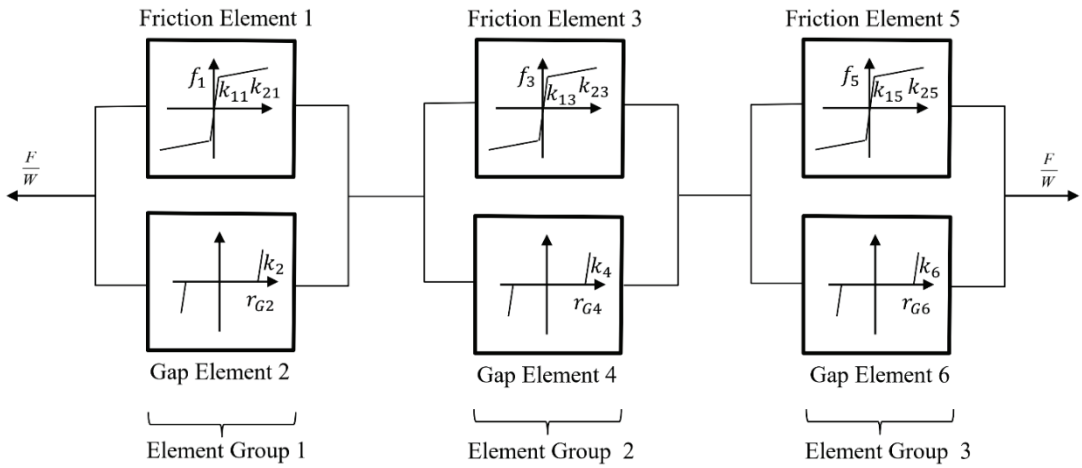

b)

Fig. 2. Numerical simulation of TFP bearings: a) force-displacement behavior for TFP bearings, b) Numerical series model for multi-stage behavior of TFP bearings

The effective period T_{eff} and damping ratio ζ_{eff} are given as [8], [9]:

(2.1) $$T_{eff} = 2\pi\sqrt{\frac{W}{k_{eff}g}}$$

and

(2.2) $$\zeta_{eff} = \frac{E_{loop}}{2\pi k_{eff}D^2}$$

where:

W – the structural weight on the isolator, E_{loop} – the energy dissipated in each cycle of the isolator, k_{eff} – the effective linear stiffness, D – the maximum displacement of the isolator under the specified level of motion.

Under the assumption that two inner sliding surfaces have identical properties and the two outer sliding surfaces have the same radius of curvature, the formula of T_{eff} can be simplified as:

(2.3) $$T_{eff} = 2\pi\sqrt{\frac{2DL_3}{[D + 2\mu_3(L_3 - L_1) - 2\mu_1 L_1]g}}$$

Buildings with single-layer or multi-layer isolation systems under vertical ground motions are investigated in this paper. The structure without TFP bearings is defined as Model 0. Four single-layer isolation forms, which are isolation at the base (Model 1), at the top of first story (Model 2), at the mid-height (Model 3), at the top of fifth floor (Model 4), are shown in Fig. 3a, b, c, d. Two multi-layer isolation schemes with isolation systems at the base and the mid-height (Model 5), and at the base, the mid-height and the top of fifth floor (Model 6) are illustrated in Fig. 3e, f.

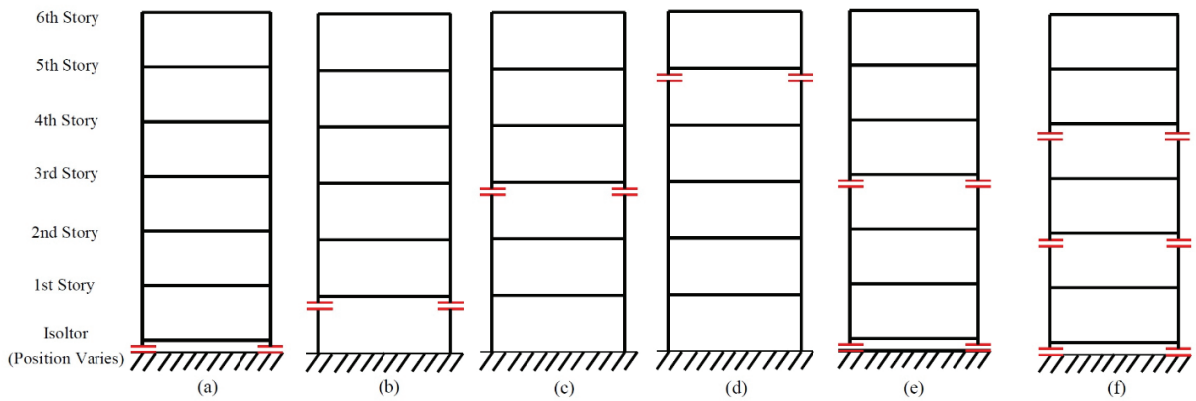

Fig. 3. Different isolation forms of isolation systems

For simplicity, the two-dimensional plane frame model of a six-story building is established and analyzed in the finite element structural analysis program OPENSEES as showed in Fig. 4a, whose frame span is 8m and story height is 3.5m. The concrete beams and columns with the sectional size to be 1×1 m and 0.3×0.8 m are modeled using a linear elastic beam-column element. The elastic modulus is 3.25×10^4 MPa and the density is 2440 kg/m^3 for the concrete. Regarding to the damping model, strictly speaking, there will be three separate parts with different damping ratios (TFP bearings, part of the building under the TFP bearings, part of the building above TFP bearings) in an interlayer isolation structure. The damping ratio of TFP bearings, listed in Table 1 and Eq. (2.2), is directly modeled by "triple friction pendulum" element. However, it is a tough task to get the exact damping ratio values for the latter two parts, since the damping ratio values may vary when the TFP bearings are set at different floors. It is simplified if the damping ratio of these two parts are both represented by a global one [3], [5], [6], [7]. Hence the damping in the interlayer isolation structure is assumed to consist of only two parts for simplicity: the damping of the TFP bearings and the damping of the structure without TFP bearings. The latter is simulated by the Rayleigh damping model. The critical Rayleigh damping ratio of 5% is assigned in the first and third models of the structures without TFP bearings based on the model analysis. The detailed structure of the story-isolation system and the assignment of the mass are shown in Fig. 4b), where isolation bearings are located at the isolator layer between the upper floor and the lower floor, and the additional mass m_a produced by the isolation devices at the isolation layer is also set to be m [1]. The TFP bearing is inserted into the numerical model as shown in Fig. 4c), where the two ends of the upper and lower column are connected by the TFP element through fixed joints. A model analysis is conducted on the structures with different isolation forms before the time-history analysis and the results of vibration period and frequency (T_s and f_s) are shown in Table 2.

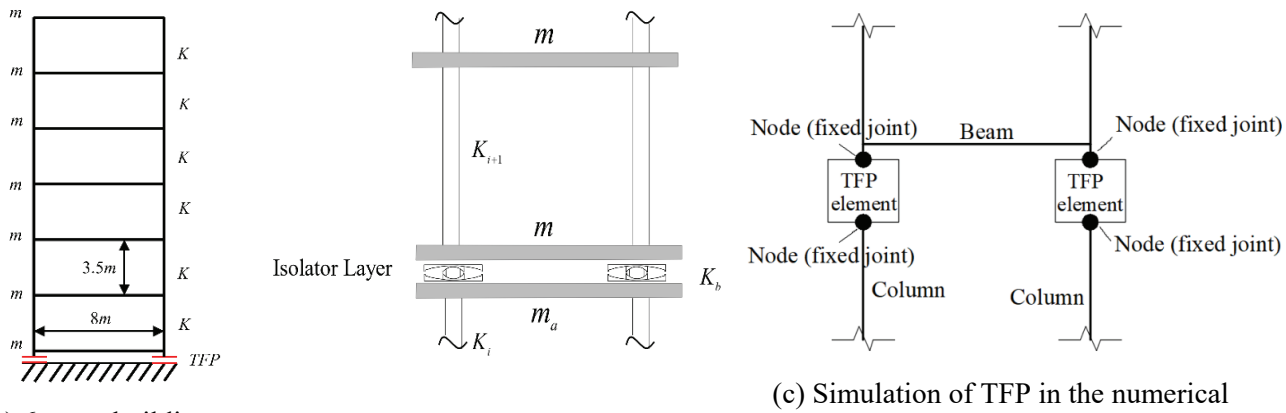

(a) 6-story building (b) Distribution of mass (c) Simulation of TFP in the numerical model

Fig. 4. Structure and isolation system

Table 2. Natural vibration period and frequency of seven models

	Model 0	Model 1	Model 2	Model 3	Model 4	Model 5	Model 6
T_s (s)	0.647	0.821	0.724	0.739	0.768	0.907	0.975
f_s (Hz)	1.546	1.218	1.381	1.353	1.302	1.103	1.026

Table 3. Characteristics of earthquake records

No.	Earthquake	Motion type	M_w	Station	A-H (g)	A-V (g)	A-V/A-H
1	San Fernando	FF	6.61	Lake Hughes #1	0.15	0.11	0.73
2	Loma Prieta	FF	6.93	Hollister-South & Pine	0.37	0.2	0.54
3	Chuetsu-oki	FF	6.8	Joetsu Kita	0.09	0.04	0.44
4	Chuetsu-oki	FF	6.8	Joetsu City	0.21	0.05	0.24
5	Chuetsu-oki	FF	6.8	NIG021	0.22	0.06	0.27
6	Darfield_ New	FF	7	Heathcote Valley Primary School	0.58	0.3	0.52
7	Imperial Valley-06	NF	6.53	Bonds Corner	0.6	0.53	0.88
8	Landers	NF	7.28	Lucerne	0.73	0.82	1.12
9	Northridge-01	NF	6.69	Newhall-Fire Sta	0.58	0.55	0.95
10	Chi-Chi	NF	7.62	TCU052	0.36	0.2	0.56
11	Chi-Chi	NF	7.62	TCU065	0.79	0.26	0.33
12	Chi-Chi	NF	7.62	TCU067	0.5	0.24	0.48

A total of 12 ground records covering a wide range of frequency contents, time durations and displacement amplitudes are considered and they are divided into two sets of six motions, representing far-field (FF) ground motions and near-fault (NF) ground motions respectively. The 12 ground records are natural accelerograms (acceleration time-history) recorded at stations during historical earthquakes and selected from the databases of Pacific Earthquake Engineering Research Center (PEER). Each ground record contains the accelerograms in both the horizontal direction and the vertical direction. The details of these records are listed in Table 3, where the motion type (far-filed FF or near-fault NF), magnitude of the earthquake M_w and the peak ground accelerations in horizontal and vertical directions (A-H and A-V) are all listed. The ratio of the peak ground acceleration in the vertical direction to that in the horizontal direction (A-V/A-H) for each record is also given. The time-history analysis is conducted using the above-mentioned finite element models of the six-story seismic isolation building. The accelerograms of the 12 ground records are exerted on finite element models in the form of inertial forces.

3. Numerical results

The responses of six-story seismic isolation buildings are investigated by the interlayer displacement, the interlayer acceleration and the interlayer shear force, since the previous one reflects the deformation of the structure and the other two indexes indicate the exerted forces to the structure from the earthquake excitations. An discrepancy rate function is adopted as shown in Eq. (3.1) to reflect the influence of vertical ground motions on structures, similar to the error function in the work by Loghman et al. [7], where R_1 is the response under one seismic component and R_2 is that under two seismic components (considering the vertical component effect). After the calculation of the discrepancy rate under each record, the average value of discrepancy rates under the twelve records are obtained. It is worth noticing that the absolute value of the discrepancy rate will be used to compare the above mentioned effect, where the story displacement discrepancy rate D_d, the story acceleration discrepancy rate D_a and the story shear discrepancy rate D_s will all be discussed.

$$\mathrm{Dis}(\%) = (R_1 - R_2)/R_2 \tag{3.1}$$

3.1. Story isolation form

The isolated period is set to be 4.5s and the friction coefficients of inner (Surface 1 and 2) and outer (Surface 3 and 4) sliding surfaces are all assumed to be constant, indicated as $f_1 = f_2 = 0.02$, $f_3 = f_4 = 0.08$. Fig. 5a, b shows the story displacement discrepancy rate of the isolation systems under the far-field and near-fault ground motions. It is observed that the story displacement discrepancy rate is generally ignorable both under the far-field and near-fault ground motions due to the negligible effect of the vertical seismic component on the story displacement. However, what needs to receive greater attention is that the story displacement discrepancy rate changes greatly at the corresponding isolation layer in both the single-layer and multi-layer isolation system. For example, the discrepancy rate of the first story in the 1st layer isolation system is greatly different from that in the other stories, and discrepancy rate changes greatly in the middle story and the 5th story respectively in the middle layer isolation system and the 5th layer isolation system. This phenomenon stems from the fact that the isolation layer divides the building into two different systems (isolation system and non-isolated system). It will be found in the following context that this phenomenon also exists in acceleration and story shear responses.

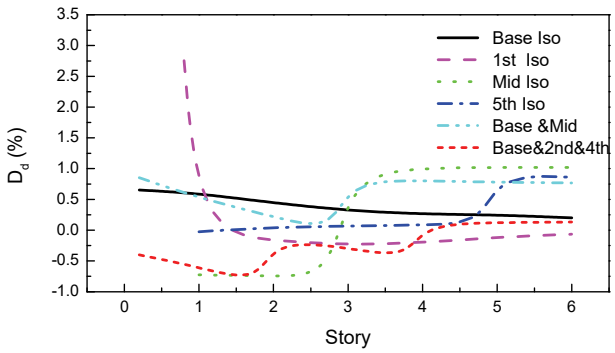

(a) Displacement discrepancy rate (far-field motion)

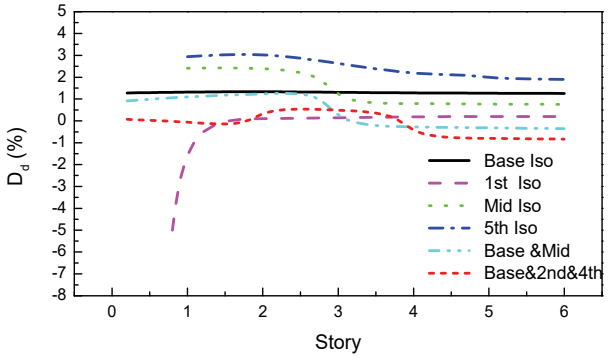

(b) Displacement discrepancy rate (near-fault motion)

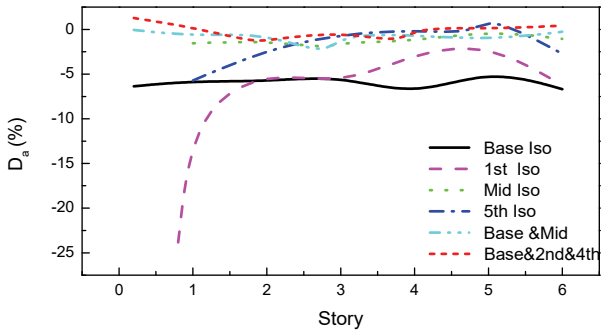

(c) Acceleration discrepancy rate (far-field motion)

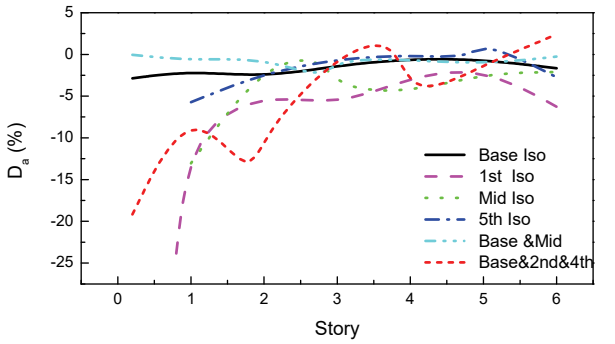

(d) Acceleration discrepancy rate (near-fault motion)

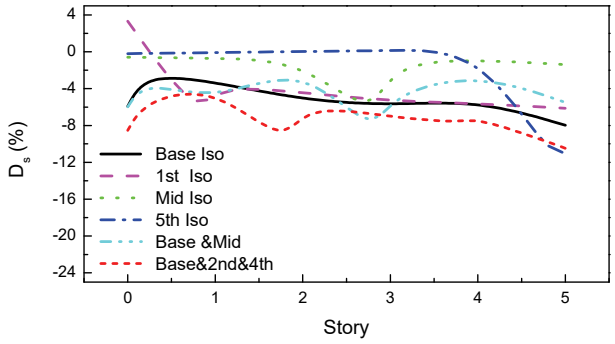

(e) Shear discrepancy rate (far-field motion)

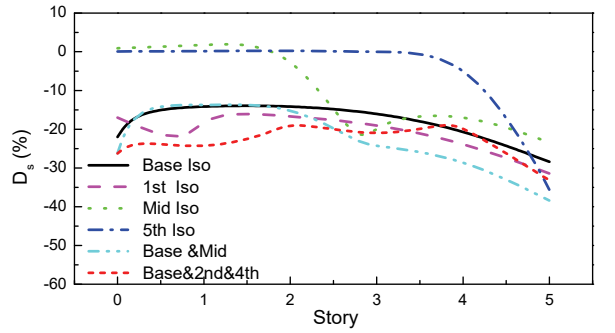

(f) Shear discrepancy rate (near-fault motion)

Fig.5. Effect of isolation forms on story displacement, acceleration and shear discrepancy rate

Based on this phenomenon, it is clear that the variation of the isolation forms will give rise to great changes of the vertical seismic effect on the displacement responses especially in the isolation layer. For example, on the first story, the displacement discrepancy rate of the 1st layer isolation structure is 2.7% while that of the 5th layer isolation structure is almost 0.

The story acceleration discrepancy rate of the single-layer and multi-layer isolation systems under the far-field and near-fault ground motions is illustrated in Fig. 5c, d. Under the far-field earthquake, the story acceleration discrepancy rate of the single-layer and multi-layer isolation system is negligible except in the case of the 1st layer isolation system, where the maximum

acceleration discrepancy rate is 24.5% on the first story. On the other hand, the story acceleration discrepancy rate becomes greater under near-fault motions, where it reaches more than 15% in half of the systems. Meanwhile, with the increase of the story number, the story acceleration discrepancy rate generally decreases. For the base isolation structures, the story acceleration discrepancy rate is negligible both under near-fault and far-field ground motions.

The maximum story acceleration discrepancy rate of the 1st layer isolation structure (24.5%) is larger than that of the middle layer isolation structure (13.8%), the 5th layer isolation structure (6.3%) and the base insolation structure (2.7%) in near-fault ground motions. It can be concluded that when the isolation devices are set on upper stories in isolation structures, the story acceleration discrepancy rate will decrease in the single-layer isolation system, indicating that the vertical seismic component plays less vital roles but they are still greater than that in the base isolation structure. For the multi-layer isolation systems, the maximum story acceleration discrepancy rate of the three-layer isolation structure (18.6%) is larger than that of the two-layer isolation structure (3.5%) and the base isolation structure (3.2%) in near-fault ground motions. It is obvious that when more isolation layers are designed on isolation structures, the story acceleration discrepancy rate will tend to increase and the vertical seismic component plays more vital roles. Similar with the trend in displacement responses, the variation of isolation forms will give rise to great changes of the vertical seismic effect on the acceleration responses especially in the isolation layer.

The story shear discrepancy rate of isolation systems under far-field and near-fault ground motions is plotted in Fig.5(e)(f). It is found that the story shear discrepancy rate is quite large under near-fault motions, where the maximum value reaches or exceeds almost 20% in most of the systems, indicating that the vertical seismic component plays an important role in the story shear responses of isolation structures. Meanwhile, it is found that the story shear discrepancy rate is also sensitive to the change of isolation forms. For example on the first story under the near-fault ground motions, the shear discrepancy rate of the 1st layer isolation structures is 20%, that of the base & 2nd & 4th layer isolation structure is 25%, while that of the 5th layer isolation structure is almost 0. Regarding to the single-layer isolation system, the story shear discrepancy rate increases as the story number increases and tends to be even larger in the multi-layer systems.

Based on the above analysis, it is clear to summarize that: (1) The influence of the vertical seismic component will contribute more to the responses of seismic isolation structures under near-fault ground motions compared with those under far-field ground motions; (2) The influence of the vertical seismic component is considerable on the acceleration and story shear responses of isolation structures, while it is negligible on the displacement responses, so in general the vertical

seismic component should not be overlooked during the design of isolation structures; (3) The influence of the vertical seismic component on the response of single-layer and multi-layer isolation structures will become greater in the isolation layer, sometimes even much greater than those of the base isolation structures, so it is advisable to consider the influence of the vertical seismic component especially at the isolation layer in isolation structures; (4) The change of isolation forms will greatly affect the influence of the vertical seismic component on the structural responses especially on the isolation layer. Isolation systems with isolation devices set on higher stories or with less isolation layers will have less vertical seismic component effect on story acceleration; (5) The seismic vertical component's effect on the story shear is obvious in the multi-layer system while it is negligible on lower stories but becomes obvious on upper stories in single-layer isolation systems, so the overlook of the vertical component effect would result in an underestimation of the structural story shear force.

3.2. Isolation period

From the above analysis, it is found that the influence of the vertical seismic component on responses of seismic isolation structures is much larger under near-fault ground motions compared with those negligible ones under far-field ground motions, and meanwhile, the influence of the vertical seismic component is also negligible on the displacement responses, so in the following context, the cases under far-field ground motions and the index of displacement will not be discussed any more.

Fig. 6 shows the influence of the isolation period on the peak story acceleration discrepancy rate. The peak story acceleration discrepancy rate is considerable since the maximum story acceleration discrepancy rate are –12% (base isolation), –20% (1st layer isolation), –15% (middle layer isolation), –18% (5th layer isolation), –25% (base &mid layer isolation) and –40% (base & mid &5th layer isolation). The peak story acceleration discrepancy rate is greatly affected by the isolation period. For instance, in the 1st layer isolation structure, the story acceleration discrepancy rate of the isolation layer is –20% (T_I = 2.5 s), –18% (T_I = 3.5 s), –15% (T_I = 4.5 s), –10% (T_I = 5.5 s). This figure shows that with the increase of the isolation period, the story acceleration discrepancy rate generally decreases especially in multi-layer isolation systems with a isolation period less than 3.5 s.

Fig.7 depicts the influence of the isolated period on the peak story shear discrepancy rate of isolation systems. This figure confirms the significant effect of the vertical seismic component on the peak story shear discrepancy rate of the isolation systems under near-fault ground motions. Meanwhile it shows the trend that most of the story shear discrepancy rate shows a fluctuating trend before it finally decreases with the increase of the isolation period.

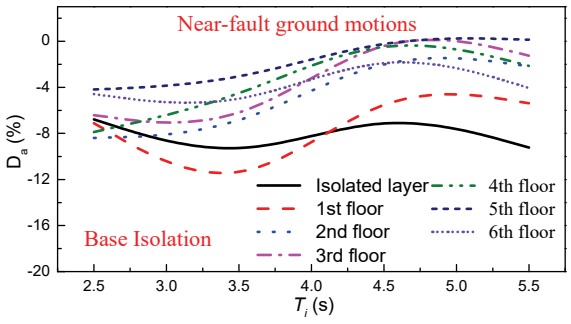

(a) Base isolation system (Model 1)

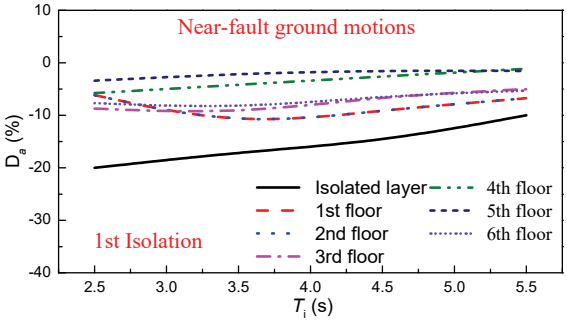

(b) 1st story isolation system (Model 2)

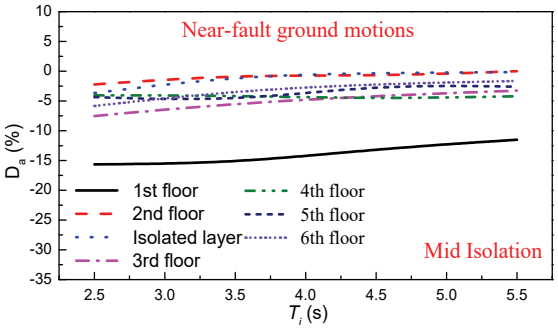

(c) Mid-story isolation system (Model 3)

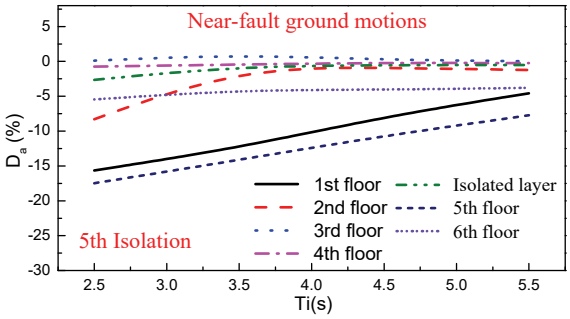

(d) 5th story isolation system (Model 4)

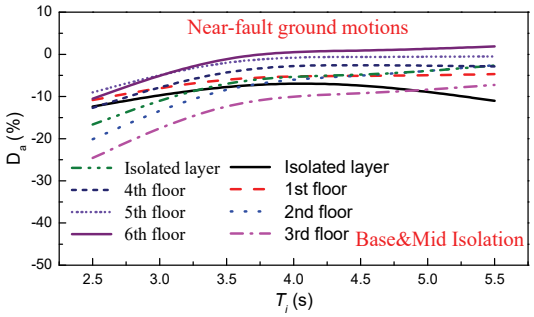

(e) Base & mid-story isolation system (Model 5)

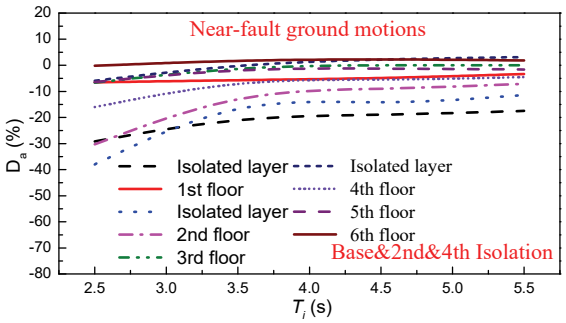

(f) Base & 2nd & 4th story isolation system (Model 6)

Fig. 6. Effect of isolation period on story acceleration discrepancy rate under near-fault ground motions

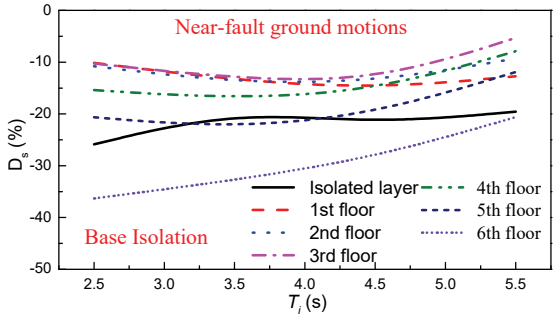

(a) Base isolation system (Model 1)

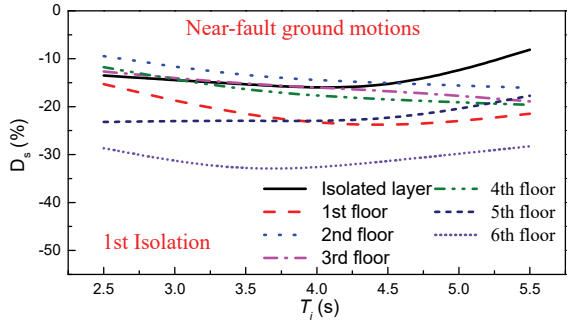

(b) 1st story isolation system (Model 2)

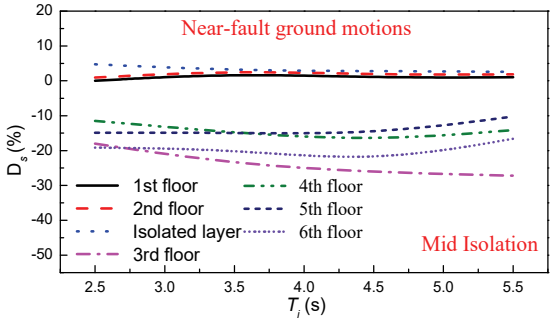

(c) Mid-story isolation system (Model 3)

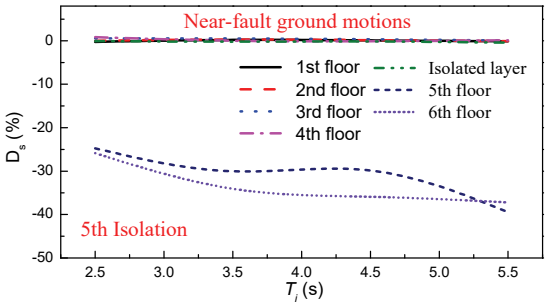

(d) 5th story isolation system (Model 4)

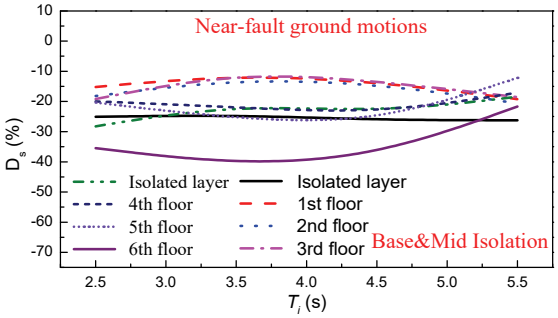

(e) Base & mid-story isolation system (Model 5)

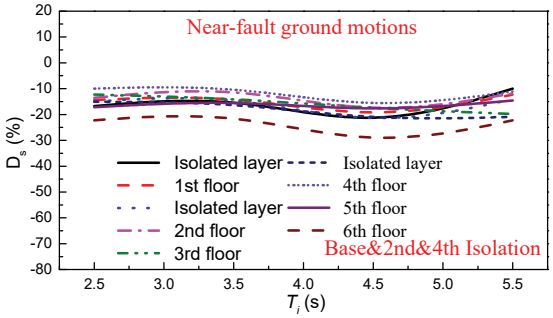

(f) Base & 2nd & 4th story isolation system (Model 6)

Fig. 7. Effect of isolation period on story shear discrepancy rate under near-fault ground motions

Based on the above analysis, it is clear to summarize that, generally speaking, the increase of the isolation period will result in the decrease of the vertical seismic component's effect on response results, although in some cases, it shows some sort of fluctuation before the final decrease.

3.3. Friction coefficient

The friction coefficient has a great effect on mechanical properties of the TFP bearings [8], [9]. In order to assess the effect of the friction coefficient, the friction coefficient for the outer top surface (surface 3) and the outer bottom surface (surface 4) has been changed from 0.02 to 0.08.

Fig. 8 and Fig. 9 shows the influence of the friction coefficient on the peak story acceleration discrepancy rate and peak shear discrepancy rate. The neglect of the vertical seismic component gives rise to a significant variation of the discrepancy rate results in the maximum story acceleration. For the single-layer isolation system and the base isolation system, the peak story acceleration discrepancy rate gradually decreases with the increase of the friction coefficient until a relatively stable value is reached. However, regarding to most multi-layer isolation systems, the peak story acceleration discrepancy rate does not tend to change noticeably with the increase of the

friction coefficient. It is also found from Fig. 9 that the story shear discrepancy rate shows this similar trend.

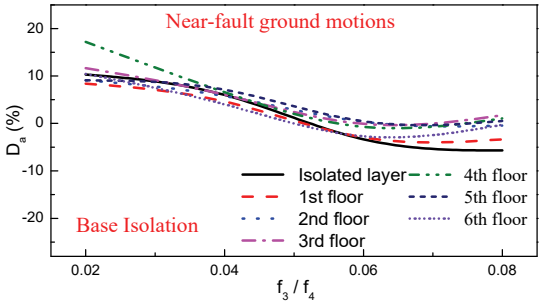

(a) Base isolation system (Model 1)

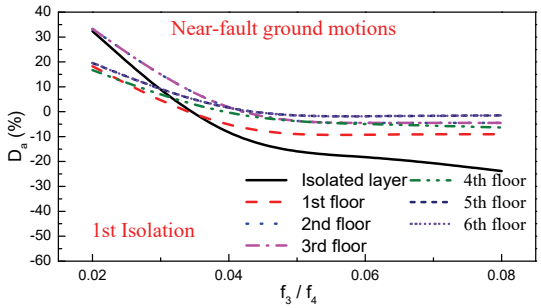

(b) 1st story isolation system (Model 2)

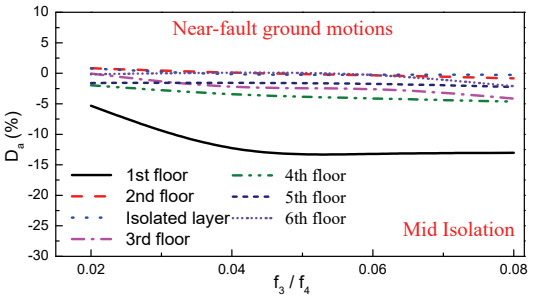

(c) Mid-story isolation system (Model 3)

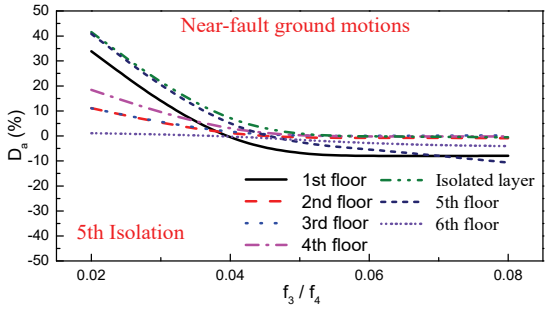

(d) 5th story isolation system (Model 4)

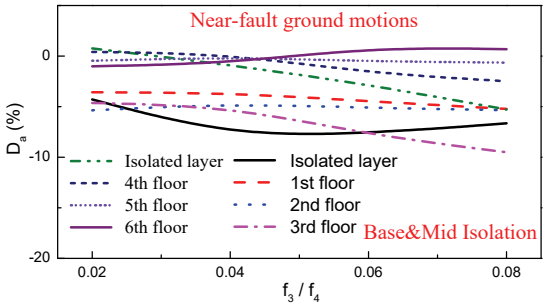

(e) Base & mid-story isolation system (Model 5)

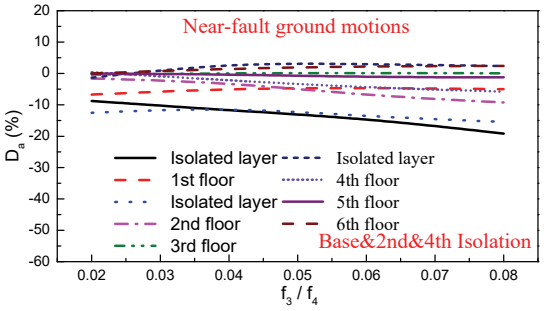

(f) Base & 2nd & 4th story isolation system (Model 6)

Fig. 8. Effect of friction coefficient on story acceleration discrepancy rate under near-fault ground motions

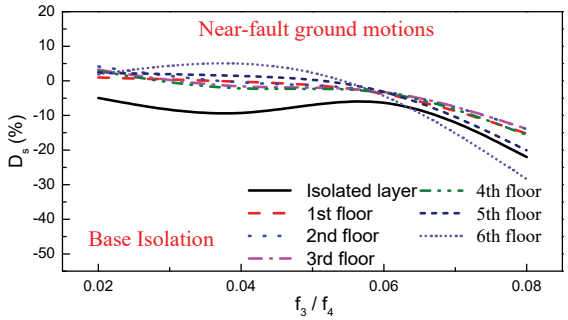

(a) Base isolation system (Model 1)

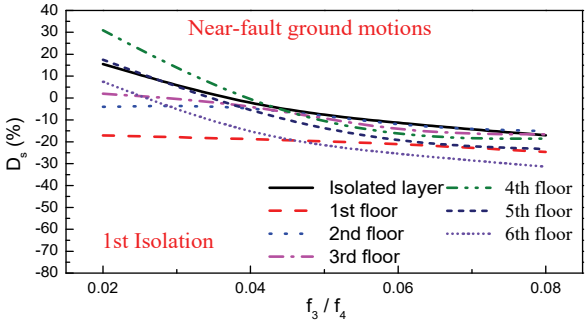

(b) 1st story isolation system (Model 2)

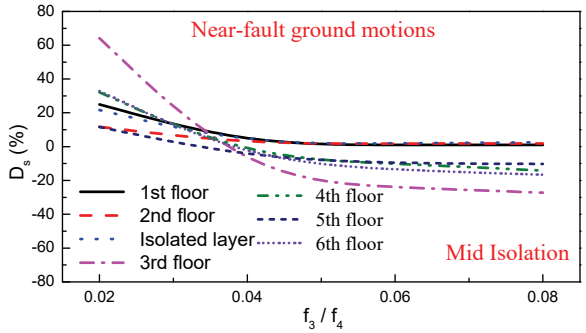

(c) Mid-story isolation system (Model 3)

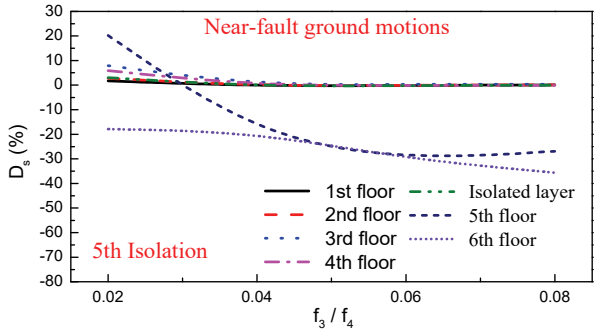

(d) 5th story isolation system (Model 4)

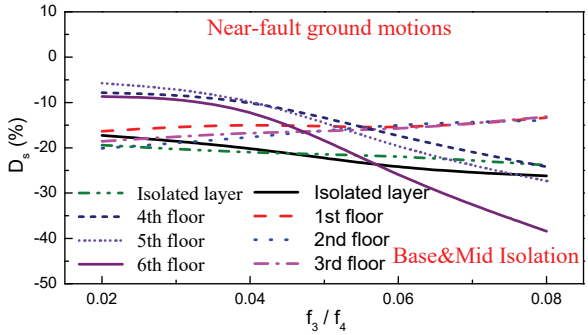

(e) Base & mid-story isolation system (Model 5)

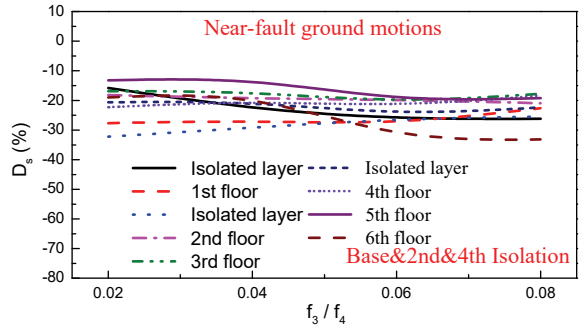

(f) Base & 2nd & 4th story isolation system (Model 6)

Fig. 9. Effect of the friction coefficient on story shear discrepancy rate under near-fault ground motions

Based on the above analysis, it is concluded that, generally speaking, in most cases of single-layer isolation systems, the increase of the friction coefficient will result in the global decrease of the vertical seismic component's effect on the structural responses, while it does not obviously affect the responses in most multi-layer isolation systems.

4. Conclusions

1) Compared with the near-fault ground motions, the influence of the vertical seismic component on the responses of isolation structures is negligible under the far-field ground motions but considerable under the near-fault ground motions.
2) The influence of the vertical seismic component on the responses of single-layer and multi-layer isolation structures will become greater on the corresponding isolation layer, sometimes much greater than those of the base isolation structures, so it is advisable to consider the influence of the vertical seismic component especially on the isolation layer in isolation structures.

3) Isolation forms greatly affect the vertical seismic component's effect on the structural responses especially on the isolation layer and isolation systems with isolation devices set on higher stories or with less isolation layers have less vertical seismic component effect on story acceleration.
4) The increase of the isolation period will generally result in the decrease of vertical seismic component's effect on response results, except in some cases the peak story shear response shows some sort of fluctuation before the final decrease.
5) Generally speaking, the increase of the friction coefficient will result in the global decrease of the vertical seismic component effect on the structural responses in single-layer isolation structures, while it does not obviously affect the responses in the multi-layer isolation system.

Acknowledgements:

The authors would like to express appreciation of the support from the National Natural Science Foundation of China (No.52008202), the Scientific Research Foundation of Nanjing Institute of Technology (YKJ201927) and the Natural Science Foundation of Jiangsu Province in China (No. BK20191016).

References

[1] K. Ryan, C. Earl. "Analysis and Design of Inter-story Isolation Systems with Nonlinear Devices," *Journal of Earthquake Engineering* 14(7): pp. 1044–1062, 2010. https://doi.org/10.1080/13632461003668020
[2] D.C.Charmpis, P.Komodromos, M.C.Phocas. "Optimized earthquake response of multi-storey buildings with seismic isolation at various elevations," *Earthquake Engineering & Structural Dynamics* 41(15): pp. 2289–2310, 2012. https://doi.org/10.1002/eqe.2187
[3] H. Fakhri, G.G. Amiri. "Nonlinear Response-History Analysis of Triple Friction Pendulum Bearings (TFPB), Installed Between Stories," 15th World Conference on Earthquake Engineering, Lisbon, 2012.
[4] A. Reggio, M.D. Angelis. "Optimal energy-based seismic design of non-conventional Tuned Mass Damper (TMD) implemented via inter-story isolation," *Earthquake Engineering & Structural Dynamics* 44(10): pp. 1623–1642, 2015. https://doi.org/10.1002/eqe.2548
[5] M. Rabiei, F. Khoshnoudian. "Response of multistory friction pendulum base-isolated buildings including the vertical component of earthquakes," *Canadian Journal of Civil Engineering* 38(10): pp. 1045–1059, 2011. https://doi.org/10.1139/l11-064
[6] K. Faramarz, R. Montazar. "Seismic Response of Double Concave Friction Pendulum Base-Isolated Structures Considering Vertical Component of Earthquake," *Advances in Structural Engineering* 13(1): pp. 1–14, 2010. https://doi.org/10.1260/1369-4332.13.1.1
[7] V. Loghman, F. Khoshnoudian, M. Banazadeh. "Effect of vertical component of earthquake on seismic response of triple concave friction pendulum base-isolated structures," *Journal of Vibration & Control* 21(11): pp. 2099–2113, 2013. https://doi.org/10.1177/1077546313503359
[8] D.M. Fenz, M.C. Constantinou. "Spherical sliding isolation bearings with adaptive behavior: Theory," *Earthquake Engineering and Structural Dynamics* 37(2): pp. 163-183, 2008. https://doi.org/10.1002/eqe.751
[9] D.M. Fenz, M.C. Constantinou. "Spherical sliding isolation bearings with adaptive behavior: Experimental verification," *Earthquake Engineering & Structural Dynamics* 37(2): pp. 185–205, 2010. https://doi.org/10.1002/eqe.750

[10] N.D. Dao. “Seismic Response of a Full-scale 5-story Steel Frame Building Isolated by Triple Pendulum Bearings under Three-Dimensional Excitations,” Dissertations & Theses - Gradworks, University of Nevada, 2012.
[11] T.C. Becker, S.A. Mahin. “Approximating peak responses in seismically isolated buildings using generalized modal analysis,” *Earthquake Engineering & Structural Dynamics* 42(12): pp. 1807–1825, 2014. https://doi.org/10.1002/eqe.2299
[12] J. Sheller, M.C. Constantinou. “Response history analysis of structures with seismic isolation and energy dissipation systems: verification examples for program SAP2000,” Report No. MCEER 99-02, Multidisciplinary Center for Earthquake Engineering Research, New York, 1999.
[13] W.I. Liao, C.H. Loh, S. Wan. “Earthquake responses of RC moment frames subjected to near-fault ground motions,” *Structural Design of Tall & Special Buildings* 10(3): pp. 219–229, 2001. https://doi.org/10.1002/tal.178

Received: 2021-02-25, Revised: 2021-05-03